Quantum Electronics **44** (4) 353–361 (2014)

LASER SPECTROSCOPY

PACS numbers: 42.62.Fi
DOI: 10.1070/QE2014v044n04ABEH015332

Recording of absorption spectra by a three-beam integral technique with a tunable laser and external cavity

P.V. Korolenko, I.V. Nikolaev, V.N. Ochkin, S.N. Tskhai

Abstract. **An integral method is considered for recording absorption using three laser beams transmitted through and reflected from an external cavity with the absorbing medium (R-ICOS). The method is the elaboration of a known single-beam ICOS method and allows suppression of the influence of radiation phase fluctuations in the resonator on recording weak absorption spectra. First of all, this reduces high-frequency instabilities and gives a possibility to record spectra during short time intervals. In this method, mirrors of the resonator may have moderate reflection coefficients. Capabilities of the method have been demonstrated by the examples of weak absorption spectra of atmospheric methane and natural gas in a spectral range around 1650 nm. With the mirrors having the reflection coefficients of 0.8–0.99, a spectrum can be recorded for 320 μs with the accuracy sufficient for detecting a background concentration of methane in atmosphere. For the acquisition time of 20 s, the absorption coefficients of $\sim 2\times 10^{-8}$ cm^{-1} can be measured, which corresponds to a 40 times less molecule concentration than the background value.**

Keywords: *tunable laser, spectroscopy, trace gas concentration, resonance cells, fast spectrum recording.*

1. Introduction

Optical methods for detecting low contents of impurities in various media including atmosphere by their capability to absorb laser radiation have been actively developing for a long time. The following tendencies have been revealed in this activity. First, frequency tunable lasers are more often used than lasers with a fixed frequency, which provides a more flexible analysis of weak atomic and molecular transitions, measurements of composition of various mixtures and multicomponent media in recording and identifying fragments of absorption spectra. Among tunable lasers, diode injection lasers are more convenient because they have small energy consumption and dimensions. Second, trace methods of laser sensing are replaced, where possible, by methods providing a longer optical path in a local domain of multipass optical cells.

Primarily, classical cells were used (and still are used) of White, Herriott, Chernin, etc. types (see, for example, [1]). In such cells, trajectories of rays multiply reflected from mirrors are separated, and in the first approximation resonance eigenfrequencies of the resonator are not revealed.

Presently, more attention is paid to cells in the form of optical resonators which were first employed in Ref. [2] for measuring parameters of highly reflecting mirrors by the rate of attenuation of short radiation pulses propagating between the mirrors. Later this idea was generalised to the case of measuring light losses inside a resonator due to absorption of radiation by intracavity medium and became widely used in absorption spectroscopy as the method of cavity ring down spectroscopy (CRDS) (see, for example, [3]). In recent years, optical schemes based on this idea have been developed for measuring absorption by observing the amplitude [3] or phase (phase shift CRDS, PS-CRDS) [4] of radiation inside the resonator. Most widespread became the variant where a cw laser was used instead of a pulsed one and in the process of frequency tuning the intensity of radiation leaving the resonator was measured. Essentially, the latter technique does not differ much and is called cavity enhanced absorption spectroscopy (CEAS) [5] or integrated cavity output spectroscopy (ICOS) [6]. We will use the latter term.

In the mentioned variants of the method, a general problem is matching the spatial beam profiles and the frequency of incident radiation with resonator eigenmodes. This is especially important in axial schemes where cell resonances correspond to maximal high-Q TEM$_{mn}$ modes with small numbers n of the transverse index; in this case, an accidental mismatch may cause intensity fluctuations of detected light passed through the resonator as high as almost 100%.

Various methods were suggested for weakening the effect of such fluctuations. An obvious approach is a long acquisition time of the detected signal. However, in this case in addition to a slow response time of the absorption recording system the result is limited by the error related to a long-term instability of probe radiation intensity or to a drift of the recording system as a whole. The time of averaging fluctuations related to matching between the radiation and resonator eigenmodes can be reduced by modulating the resonator length by piezoelectric actuators [7]. One more method is based on abandoning axial input of radiation into a resonator. In the latter case, resonator modes with high transverse mode numbers n are used, which have a dense spectum of eigenfrequencies [8]. The matching effects are noticeably suppressed; however, resonance properties of the resonator worsen and it

P.V. Korolenko P.N. Lebedev Physics Institute, Russian Academy of Sciences, Leninsky prosp. 53, 119991 Moscow, Russia; Department of Physics, M.V. Lomonosov Moscow State University, Vorob'evy gory, 119991 Moscow, Russia; e-mail: pvkorolenko@rambler.ru;
I.V. Nikolaev, S.N. Tskhai P.N. Lebedev Physics Institute, Russian Academy of Sciences, Leninsky prosp. 53, 119991 Moscow, Russia; e-mail: primobaler@mail.ru;
V.N. Ochkin P.N. Lebedev Physics Institute, Russian Academy of Sciences, Leninsky prosp. 53, 119991 Moscow, Russia; Moscow Institute of Physics and Technology (State University), Institutskii per. 9, 141700 Dolgoprudnyi, Moscow region, Russia;
e-mail: ochkin@sci.lebedev.ru

Received 25 October 2013; revision received 16 December 2013
Kvantovaya Elektronika **44** (4) 353–361 (2014)
Translated by N.A. Raspopov

becomes similar to classical resonators. In addition, the intensity of detected radiation is substantially lower than in the scheme with axial radiation input [9, 10]. One may conclude that the problem of suppressing fluctuations has been known for long; however, there is no satisfactory solution yet.

In Ref. [11] we proposed the idea of suppressing fluctuations by combining an ICOS signal with a signal of light reflected from the resonator. This improved the stability of the optical system to external perturbations, but we failed to detect weak absorption spectra [11]. The reason of such a failure found in our recent work [12] was related to a significant mismatch between the widths of the laser line and resonator modes. After eliminating this contradiction we successfully recorded spectra of weak absorption with a high signal-to-noise ratio [12].

The present work is continuation of previous purely experimental works [11, 12] and is aimed at a more thorough analysis of the R-ICOS method from the viewpoint of organising measurements and its possibilities.

2. General prerequisites for increasing the number of optical channels in the R-ICOS method as compared to the ICOS technique

2.1. Three-beam scheme

A principal optical scheme of measurements by the R-ICOS technique discussed in the present work is given in Fig. 1. Radiation of a tunable laser TL is divided by a plate P to three beams. The intensity of the beam passed through the Fabry–Perot resonator R with mirrors M1 and M2 is measured according to a conventional ICOS scheme. In our case, the intensity I_1 depends on the intensity of the initial beam I_0 and on transmissions of the plate and the resonator with absorbing medium. The intensity I_2 of the beam reflected from the plate is only proportional to the intensity of the initial laser beam I_0 (base line) and controls it in the process of tuning the generation frequency. The intensity of the third beam I_3 is determined by the reflection coefficients of the resonator and plate.

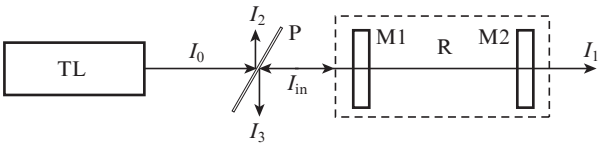

Figure 1. Optical scheme for measurements by the R-ICOS technique (see notations in the text).

Let T_c and R_c be, respectively, the transmission and reflection coefficients of the resonator having, in a general case, losses. The energy balance condition for the system is expressed by the equality

$$I_0 = I_1 + I_2 + a_3 I_3 + \Delta I. \tag{1}$$

Here ΔI is determined by losses of light in the resonator and the coefficient a_3 makes allowance for the part of radiation reflected from resonator R passing back through the plate P to the laser. We introduce the coefficients k_1, k_2, and k_3 such that $I_0 = k_2 I_2$, $I_1 = k_1 T_c I_0$, $I_3 = k_3 R_c I_0$. The coefficients k_1, k_2, and k_3 are determined by transmission and reflection of the dividing plate P. Then relation (1) takes the form

$$I_2 = \left(\frac{k_1 k_2}{k_2 - 1}\right) T_c I_2 + \left(\frac{a_3 k_1 k_2}{k_2 - 1}\right) T_c I_2 + \frac{\Delta I}{k_2 - 1}. \tag{2}$$

In a particular case of absent losses ($\Delta I = 0$) inside the resonator we have $T_c + R_c = 1$ and, consequently, the expressions in the parentheses in relation (2) are equal to unity. Relative losses Δ (the ratio of the resonator losses ΔI to the intensity $I_{in} = I_0 - I_2$ of incident radiation) are given by the expression

$$\Delta = \frac{\Delta I}{I_2(k_2 - 1)} = 1 - \frac{I_1}{I_2(k_2 - 1)} - \frac{a_3 I_3}{I_2(k_2 - 1)}. \tag{3}$$

Then in view of the fact that the expressions in parentheses in (2) are equal to unity, expression (3) takes the simple form:

$$\Delta = 1 - T_c - R_c. \tag{4}$$

The transmission and reflection coefficients of the resonator are determined by the known formulae of the Fabry–Perot interferometer [13]:

$$T_c = \frac{T_m T^2}{(1 - T_m r)^2 + 4 T_m r \sin^2 \delta}, \tag{5}$$

$$R_c = \frac{r[1 - (r + T) T_m]^2 + 4 T_m r (r + T) \sin^2 \delta}{(1 - T_m r)^2 + 4 T_m r \sin^2 \delta}, \tag{6}$$

where T_m is the transparency of a substance filling the resonator per single pass of radiation between the mirrors; r are the reflection coefficients of mirrors with respect to intensity; $T = 1 - r - a$ are the transmission coefficients of the mirrors with respect to intensity; a are losses of mirror; and δ is the phase shift attained by a monochromatic wave in a single passage over the cavity*.

Transparency of a material is determined by the Bouguer–Lambert–Beer law. If α is the absorption index of a substance between the mirrors separated by a distance L, then at $\alpha L \ll 1$ the transparency is

$$T_m = \exp(-\alpha L) \approx 1 - \alpha L. \tag{7}$$

Then, expression (3) for relative losses inside the resonator takes the form

$$\Delta = 1 - R_c - T_c \approx \frac{(1 + r)\alpha L T - r(\alpha L)^2 T}{(1 - T_m r)^2 + 4 T_m r \sin^2 \delta} \tag{8}$$

or, neglecting the terms of the second order of smallness,

* Formulae (5) and (6) for a plane-parallel Fabry–Perot interferometer may be also generalised to the case of exciting a spherical stable resonator by the axial TEM_{00}-wave matched with the fundamental mode of the resonator [9]. One should take into account that the phase shift δ which for a plane-parallel resonator is $2\pi L/\lambda$ (L is the cavity length, and λ is the wavelength), for a symmetrical spherical resonator will be determined by the expression [14] $\delta = 2\pi L/\lambda - 2\arctan[\lambda L/(2\pi w_0^2)]$ (w_0 is the radius of beam waist for the fundamental mode).

$$\Delta \approx \frac{(1+r)\alpha L T}{(1-T_m r)^2 + 4T_m r \sin^2\delta} = \frac{(1+r)\alpha L}{T}\frac{T_c}{T_m}$$

$$\approx \alpha L(1+r)\frac{T_c^*}{T}, \qquad (9)$$

where T_c^* is the resonator transmission coefficient (5) at $T_m = 1$.

2.2. Common features of the ICOS and R-ICOS methods

In a conventional ICOS scheme (Fig. 1) the intensities of the light beam I are measured in the cases of a resonator with an absorbing substance and without it. In the first case the intensity is I_1 and in the second case it is $\tilde{I}_1$, so that their difference

$$\tilde{I}_1 - I_1 = \tilde{\delta}I = I_{in}(T_c^* - T_c) \qquad (10)$$

determines the value of αL. In both the ICOS and R-ICOS schemes the absorption index is found by measuring the intensity in resonator transmission peaks ($\sin^2\delta = 0$), i.e, from the expression

$$\tilde{\delta}I = I_{in}\left[\frac{T^2}{(1-r)^2} - \frac{T^2 T_m}{(1-r+\alpha L r)^2}\right]. \qquad (11)$$

By rejecting terms small as compared to $\alpha L r/(1-r) \ll 1$ at $r \approx 1$ (which holds for all ICOS schemes) we obtain

$$\tilde{\delta}I \simeq I_{in}\frac{T^2}{(1-r)^2}\frac{2\alpha L r}{1-r} = \tilde{I}_1\frac{2\alpha L r}{1-r},$$

or

$$\alpha L = \frac{\tilde{\delta}I}{\tilde{I}_1}\frac{1-r}{2r}, \qquad (12)$$

which coincides with the results in Ref. [3].

Spectral dependences of the parameters measured by the R-ICOS and ICOS methods for the same profile $\alpha(\nu)$ of the absorption line of a substance inside the resonator are presented in Fig. 2. In both cases the absorption profile is recovered as an envelope drawn by the results of measurements of resonator transmission at the frequencies corresponding to resonance conditions ($\sin^2\delta = 0$) in formulae (5) and (6). The intensity of a passed wave is proportional to the product $T_c^*\alpha(\nu)$. In the case of ICOS, two successive measurements are needed, namely, with an absorbing material inside the resonator and without such a material. If the absorption is weak it can be found according to formula (12) from the small difference $\tilde{\delta}I$ between noticeably greater intensities $\tilde{I}_1$ and I_1 of light passed through the resonator. In the case of R-ICOS the value of Δ directly related to the absorption index is calculated by formula (3) using the three intensities of transmitted and reflected light measured simultaneously.

In typical experiments the reflection coefficients of mirrors are sufficiently high ($1 + r \approx 2$), the peak values of transmission coefficient T_c^* are close to unity and the values of signals measured at the centre of the absorption profile are actually the same in both the schemes.

In the case of a monochromatic line of illuminating radiation the spectral resolution of the R-ICOS method similarly to the axial ICOS method is determined by a free spectral interval of the resonator $\Delta\nu \approx 1/(2L)$.

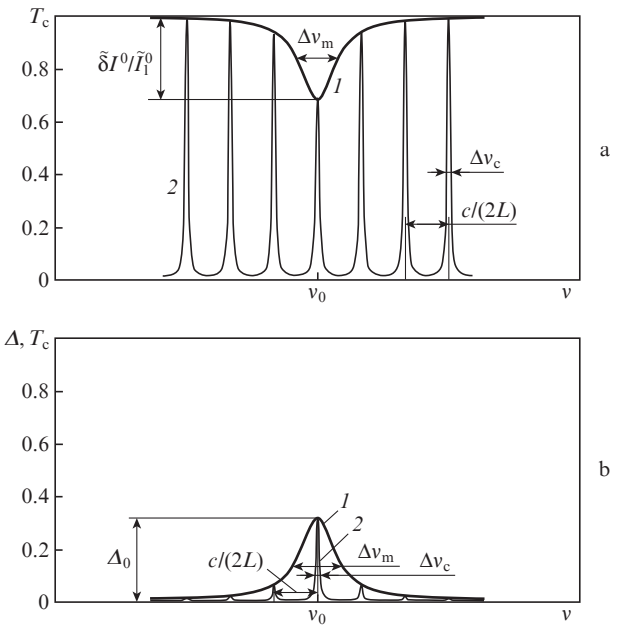

Figure 2. Spectral dependences of parameters measured by (a) the ICOS and (b) R-ICOS methods: envelopes of (*1*; a) transmission peaks and (*1*; b) losses Δ (9), (*2*) transmission coefficient of resonator T_c; $\tilde{\delta}I^0/\tilde{I}_1^0$ is the relative variation of intensities in the centre of the absorption line ($\nu = \nu_0$), $\Delta\nu_c$ is the width of the transmission peak of the resonator, $\Delta\nu_m$ is the width of the absorption line, and c is the speed of light.

2.3. Differences between the methods and their mutual complementation

In spite of the common features of the ICOS and R-ICOS methods mentioned above they differ and complement each other. The R-ICOS method introduces no substantial principal (Fig. 1) and experimental (see below) changes into the ICOS scheme.

First, note the features related to a finite spectral width of the illuminating radiation line. Let the spectral density of radiation power of a nonmonochromatic source with a central frequency ν_* be determined by the function $\varphi(\nu - \nu_*)$. Then, the intensity of a quasi-monochromatic wave in an interval $[\nu, \nu + d\nu]$ is $dI = \varphi(\nu)\,d\nu$ and, according to formulae (1), (5), and (6) we have

$$dI_1(\nu) = dI_{in}(\nu)T_c(\nu), \qquad (13)$$

$$a_3 dI_3(\nu) = dI_{in}(\nu)R_c(\nu). \qquad (14)$$

The total intensities of transmitted and reflected radiations for a line with a central frequency ν_* can be found by integrating expressions (13) and (14):

$$I_1(\nu_*) = \int dI_{in}(\nu)\,T_c(\nu) = \int_0^\infty \varphi(\nu - \nu_*)\,T_c(\nu)\,d\nu, \qquad (15)$$

$$a_3 I_3(\nu_*) = \int dI_{in}(\nu)\,R_c(\nu) = \int_0^\infty \varphi(\nu - \nu_*)\,R_c(\nu)\,d\nu, \qquad (16)$$

$$I_{in}(\nu_*) = \int dI_{in}(\nu) = \int_0^\infty \varphi(\nu - \nu_*)\,d\nu. \qquad (17)$$

The expression for the parameter αL measured by the ICOS method is obtained by repeating the actions from Section 2.2,

but with a substitution of $\tilde{I}_1$ and I_1 in (12) for the corresponding values according to formula (15). After simple transformations one can see that the expressions for the relative intensity variations of a nonmonochromatic radiation still have the same form as expressions (12) for a monochromatic radiation.

A physical sense of this result is as follows. Noncoincidence between spectral line profiles of transmitting radiation and the resonator transmission may affect the part of radiation injected into the resonator and the absolute values of intensities $\tilde{I}_1$ and I_1 may differ for different profile widths. However, this part of radiation is the same in the cases of a filled or empty resonator, because the ICOS scheme implies measurement of the relative variation in the intensity of the radiation passed through the resonator, which, in turn, is equal to the relative variation in the resonator transmission.

In the case of R-ICOS the situation is different. The variation in the part of injected radiation also changes the part of reflected radiation with an opposite sign, which should be taken into account. By repeating the considerations of Section 2.1 and using, instead of the intensities of monochromatic radiation, their analogues for a nonmonochromatic radiation determined by formulae (15), (16), and (17) we obtain the expressions for an analogue of the parameter Δ determined by (4), (8), and (9):

$$\tilde{\Delta}(\nu_*) = \frac{I_{\text{in}} - I_1 - a_3 I_3}{I_{\text{in}}} \approx \frac{\int \alpha(\nu) L(1+r)\varphi(\nu-\nu_*)\, T_{\text{c}}^*(\nu)\,\mathrm{d}\nu}{T\int \varphi(\nu-\nu_*)\,\mathrm{d}\nu}. \tag{18}$$

Usually the width of the absorption band $\alpha(\nu)$ is substantially greater than the line width of a radiation source; thus, within the interval in which the radiation intensity is distinct from zero we may consider the factor $\alpha(\nu)L(1 + r)$ constant and take it outside the integral sign. Now, the expression for $\tilde{\Delta}(\nu_*)$ takes the form

$$\tilde{\Delta}(\nu_*) \approx \frac{\alpha(\nu_*) L(1+r)\int \varphi(\nu-\nu_*)\, T_{\text{c}}^*(\nu)\,\mathrm{d}\nu}{T\int \varphi(\nu-\nu_*)\,\mathrm{d}\nu}. \tag{19}$$

If we consider a signal obtained in the R-ICOS scheme, similarly to the case of ICOS, in the centre of the resonator mode with frequency $\nu_* = \nu_{\text{c}}$ then expression (19) can be written in the form

$$\tilde{\Delta}(\nu_{\text{c}}) = \Delta(\nu_{\text{c}})\,\tilde{C} \approx \tilde{C}\alpha(\nu_{\text{c}}) L(1+r)\frac{T_{\text{c}}^*(\nu_{\text{c}})}{T}, \tag{20}$$

where the factor $\tilde{C} \leqslant 1$ determines the part of radiation injected into the resonator:

$$\tilde{C} = \frac{\int \varphi(\nu-\nu_{\text{c}})\, T_{\text{c}}^*(\nu)\,\mathrm{d}\nu}{T_{\text{c}}^*(\nu_c)\int \varphi(\nu-\nu_*)\,\mathrm{d}\nu}.$$

In the case of quasi-monochromatic radiation, $\tilde{C} = 1$ and formulae (9) and (20) coincide. For nonmonochromatic radiation this factor can be calculated. It can also be found experimentally by comparing measurement results of ICOS and R-ICOS methods if we recall that results in the ICOS method are independent of the ratio of spectral profiles of the resonator transmission and illuminating radiation. One can find the absorption index $\alpha(\nu_{\text{c}}) = \alpha_{\text{ICOS}}(\nu_{\text{c}})$ for a peak transmission ($T_{\text{c}}^* = 1$) by the ICOS method and employ formula (20) to obtain

$$\tilde{C} = \frac{T\tilde{\Delta}(\nu_{\text{c}})}{L\alpha_{\text{ICOS}}(\nu_{\text{c}})(1+r)}. \tag{21}$$

This provides a calibration procedure for an R-ICOS optical system in the case where the illuminating radiation is not monochromatic. These calibration measurements are appropriate at an elevated concentration of absorbing matter in order to minimise the influence of noise on the accuracy of determining $\tilde{C}$, because the signal-to-noise ratio may noticeably differ for the methods considered.

Consider the influence of the instability of detected signals due to random fluctuations of frequency detuning from the central frequency corresponding to the resonator peak transmission on the sensitivities of ICOS and R-ICOS methods. We may assume that in measurements of transmission and reflection coefficients, the noise is determined by random fluctuations of the phase δ included in (5) and (6). The phase fluctuations may be related to frequency fluctuations of illuminating radiation or with the mechanical instabilities of resonator which change positions of transmission peaks on the frequency axis (fluctuations of resonator transmission). We denote a variance of transmission for the resonator without an absorbing matter by $\sigma^2_{T_{\text{c}}^*}$ and with an absorbing matter by $\sigma^2_{T_{\text{c}}}$ and find the variances of absorption indices for both the schemes. We will assume that the phase fluctuations occur in a vicinity of a maximum resonator transmission where measurements are performed. We may estimate an error of measuring the absorption index α by the ICOS and R-ICOS methods.

For the ICOS scheme the variance according to formulae (10) and (12) is

$$\sigma^2_{\text{ICOS}} = \left(\frac{1-r}{2rL}\right)^2 \sigma^2 \frac{\tilde{\delta}I}{\tilde{I}_1} = \left(\frac{1-r}{2rL}\right)^2 \sigma^2\left(1 - \frac{T_{\text{c}}}{T_{\text{c}}^*}\right), \tag{22}$$

and for the R-ICOS scheme according to (9) we obtain

$$\sigma^2_{\text{RICOS}} = \left[\frac{1-r}{(1+r)L}\right]\sigma^2(\Delta) = \left[\frac{1-r}{(1+r)L}\right]\sigma^2\left[\alpha L(1+r)\frac{T_{\text{c}}^*}{T}\right]. \tag{23}$$

We may express variances (22) and (23) in terms of variances of the resonator transmission coefficients T_{c} and T_{c}^*:

$$\sigma^2_{\text{ICOS}} = \left(\frac{1-r}{2rL}\right)^2 \left\{\left(\frac{1}{\bar{T}_{\text{c}}^*}\right)\sigma^2_{T_{\text{c}}} + \left[\frac{\bar{T}_{\text{c}}}{(\bar{T}_{\text{c}}^*)^2}\right]\sigma^2_{T_{\text{c}}^*}\right\}, \tag{24}$$

$$\sigma^2_{\text{RICOS}} = \left[\frac{T}{(1+r)L}\right]^2 (1+r)^2 \left(\frac{\alpha L}{T}\right)^2 \sigma^2_{T_{\text{c}}^*} = \alpha^2 \sigma^2_{T_{\text{c}}^*}, \tag{25}$$

where $\bar{T}_{\text{c}}$ and $\bar{T}_{\text{c}}^*$ are average values of transmission coefficients at the wavelength corresponding to a centre of mode.

In view of $\alpha L \ll T \ll 1$ we may write the relationships

$$\bar{T}_{\text{c}} \approx \bar{T}_{\text{c}}^*, \tag{26}$$

$$\sigma^2_{T_{\text{c}}} \approx \sigma^2_{T_{\text{c}}^*}. \tag{27}$$

By substituting them to (24) we arrive at

$$\sigma^2_{\text{ICOS}} \approx \left(\frac{1-r}{2rL\bar{T}_{\text{c}}^*}\right)^2 2\sigma^2_{T_{\text{c}}^*}. \tag{28}$$

By using expressions (24) and (25) one may estimate a minimal ratio of variances for signals obtained by ICOS and R-ICOS methods assuming that the mirrors possess sufficient reflection coefficients ($1 + r \approx 2$), low dissipative losses ($T \approx 1 - r$), and that near the centre of the resonator mode the relations $\bar{T}_c^* \leqslant 1$ and $\alpha L \ll (1 - r) \ll 1$ hold:

$$\left(\frac{\sigma^2_{\mathrm{ICOS}}}{\sigma^2_{\mathrm{RICOS}}}\right)^{1/2} \approx \frac{\sqrt{2}\,T}{2(\alpha L)}. \qquad (29)$$

From (29) one can see that at $\alpha L \ll T \ll 1$ the value of σ_{RICOS} is substantially less than σ_{ICOS}. From expressions (9), (10), (25), and (28) it follows that if losses inside the resonator are absent, then the absorption index and its variance measured by the R-ICOS method will be definitely zero in contrast to the variance of the refraction index measured by the ICOS method that is always distinct from zero.

A physical sense of this conclusion is that in the ICOS scheme a frequency fluctuation of radiation relative to the position of the resonator peak transmission is directly converted to a fluctuation of the measured signal. However, in the R-ICOS method, transmission and reflection variations have opposite signs and compensate for each other in the detected signal Δ according to expression (4).

3. Experimental technique. Measurement method

The scheme of the experimental setup is shown in Fig. 3. Emission of a vertical cavity surface-emitting diode laser [VCSEL, Vertilas, the power of up to 1.5 mW in a spectral range ~1650 nm (6060 cm^{-1})] after passing through an optical isolator OI, matching lens L, and quartz plane-parallel dividing plate P enters the resonator R. The spectral width of the lasing line, according to producer information, is 10 MHz. The temperature of the laser housing was stabilised by a Peltier element with an accuracy of up to 10^{-3} K. The laser radiation frequency in the range of 1.15 cm^{-1} was tuned by a trapezoidal pump current pulse (see, for example, Ref. [15]). The duration of the injection current pulses varied from 320 μs to 5 ms with a duty factor of 1. A maximal value of the injection current was 4.85 mA; a minimal current was 3.93 mA. A resonator of length $L = 50$ cm was formed by two mirrors of diameter 25 mm with the radius of curvature 1 m. The mirrors had the reflection coefficients $r = 0.8$ and 0.99 at a wavelength of 1650 nm. The photo-detector of the first channel PD1, which recorded an ICOS signal, was placed behind the resonator. The laser radiation reflected from the plate (the base line signal) was recorded by a detector of the second channel PD2. The radiation reflected from the resonator by the same plate was directed onto a third-channel detector PD3. The signals from all three channels pass to an interface card NI PCI-6120 (National Instruments) for processing in a personal computer PC. The interface card was also used for controlling the injection current; hence, the intensity and frequency of laser radiation varied linearly with the current. In the case of repetitively pulsed operation, in each scanning cycle the signals from detectors were digitised with a sampling period of 1.25 μs. Usually, the entire scanning cycle comprised 4096 points except for cases of fast scanning (shorter than 1 ms) where a scan comprised only 256 points due to performance limitations of the card.

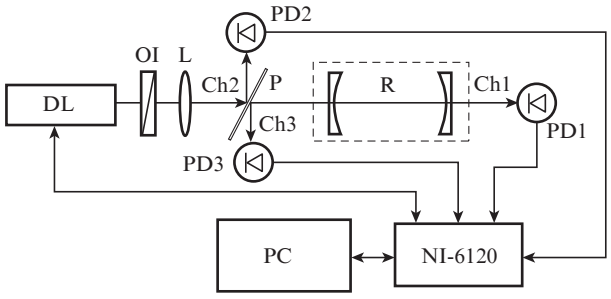

Figure 3. Schematic diagram of the experimental setup: (DL) diode laser; (L) matching lens; (OI) optical isolator; (P) plane-parallel quartz plate; (R) resonator; (PD1–PD3) photodetectors; (NI-6120) multichannel I/O card; (PC) personal computer; (Ch1) analytic channel; (Ch2) base line channel; (Ch3) reflected radiation channel.

The optical isolator OI comprised a Glan–Taylor prism and a quarter-wave plate and was used for suppressing the optical feedback caused by the radiation reflected from and scattered by optical elements back to the laser. Thorough measurements of frequency characteristics of tuned laser radiation in some experiments were performed by installing a quartz Fabry–Perot interferometer of length 10 cm in the second channel Ch2. In some experiments, the radiation frequency was controlled by placing a resonator filled with pure methane at low pressure in this channel.

Linearity of all photodetectors was verified by special measurements. Signals from photodetectors in different channels depend on detector sensitivities and parameters of the optical system. These factors were jointly taken into account by filling the resonator with pure nitrogen, in which case the selective losses due to absorption are absent. Using expression (3) in this case ($\Delta = 0$) we obtain the relation for signal values in the form

$$I_2 = p_3 I_3 + p_1 I_1,\ p_1 = 1/(k_2 - 1),\ p_3 = a_3/(k_2 - 1). \qquad (30)$$

In a comparatively narrow spectral range of laser tuning the coefficients p_i are constant. Their values can be found by measuring the intensities in all three channels. Relations of light signals in different channels depend, in particular, on the ratio of the laser line width to the width of the resonator transmission peak. For example, for mirrors with the reflection coefficients $r = 0.99$ and 0.8 in a maximum of the resonator transmission, the characteristic relations of light signals are estimated as $I_1{:}I_2{:}I_3 \approx 1{:}0.5{:}0.7$ and $I_1{:}I_2{:}I_3 \approx 1{:}0.6{:}0.3$, respectively. This problem is more thoroughly discussed in Ref. [12]. The relations of signals from detectors may differ due to distinct gains in different ADC channels. Real values of p_i with these and other factors taken into account were determined by using a linear regression procedure [15, 16] with a software from the LabVIEW 2009 package [17]. The accuracy corresponded to the condition $|\overline{I_2/(p_3 I_3 + p_1 I_1) - 1}| < 10^{-4}$, where the overline means averaging over the whole sampling set within the limits of a cycle of injection current variation (spectral scanning by tuning the laser frequency).

The regression coefficients p_i obtained in this way were employed for calculating a spectrum of gas absorption $\alpha(\nu)$ in varying the laser radiation frequency ν using formulae (3), (9) and the relationship

$$\alpha(\nu) L(1 + r)\frac{T_c^*}{T} = \frac{I_2 - p_3 I_3 - p_1 I_1}{I_2} \qquad (31)$$

in maxima of the resonator transmission, which for resonators with highly reflecting mirrors corresponds to $T_c^* \approx 1$.

Absorption measurements were performed for methane and natural gas in their mixtures with atmospheric air in controlled proportions at a total pressure of 1 atm and for methane background contents in air [18].

4. Results and discussion

Absorption spectra in the band $2\nu_3$ of the R(3) branch for CH_4 molecule (ν = 6046.9647 cm^{-1}) obtained by the R-ICOS and ICOS methods are presented in Fig. 4. Methane concentration in air was ~0.05%. In both the cases a spectrum was recorded in a single cycle of laser frequency tuning of duration 5 ms with a total number of sampling points 4096. The resonator mirrors had the reflection coefficients of 0.8. Note that in the spectra presented no structure of resonator axial modes is observed, although such a structure is predicted by the theory of ICOS and R-ICOS methods for monochromatic illuminating radiation (see Section 2 and Fig. 2). This is related, first of all, to a limited performance of photodetectors; hence, the curves presented in Fig. 4 and other figures correspond to envelopes of resonator transmission peaks, i.e., present direct absorption spectra. The mode structure of the resonator is clearly revealed at a spectrum recording time exceeding 100 ms.

The signal-to-noise ratio in the R-ICOS method is approximately 30 times greater than that in the ICOS method, and, correspondingly, the signal variance is approximately 1000 times less, including cases of fast spectrum recording. The latter is illustrated in Fig. 5 where fragments of an absorption spectrum

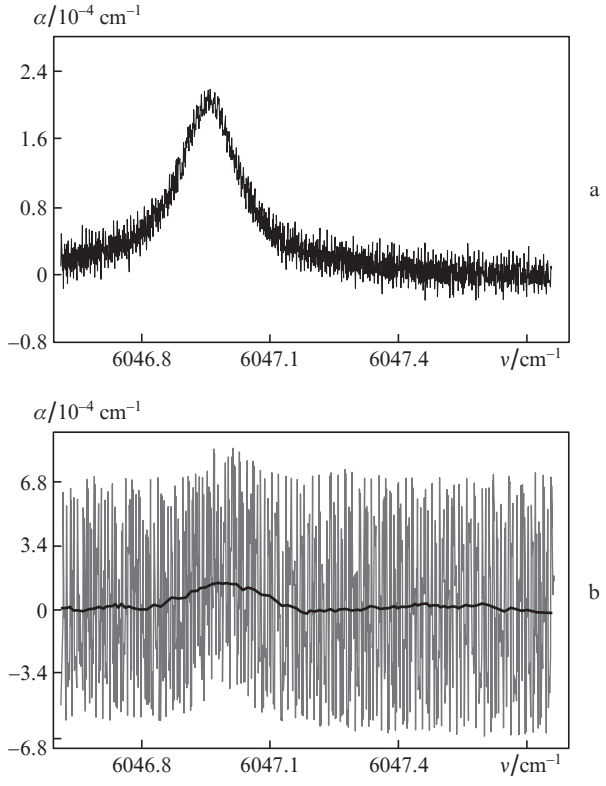

Figure 4. Methane absorption spectra recorded in a single cycle of laser frequency scanning in (a) the R-ICOS and (b) ICOS methods; the scanning time is 5 ms.

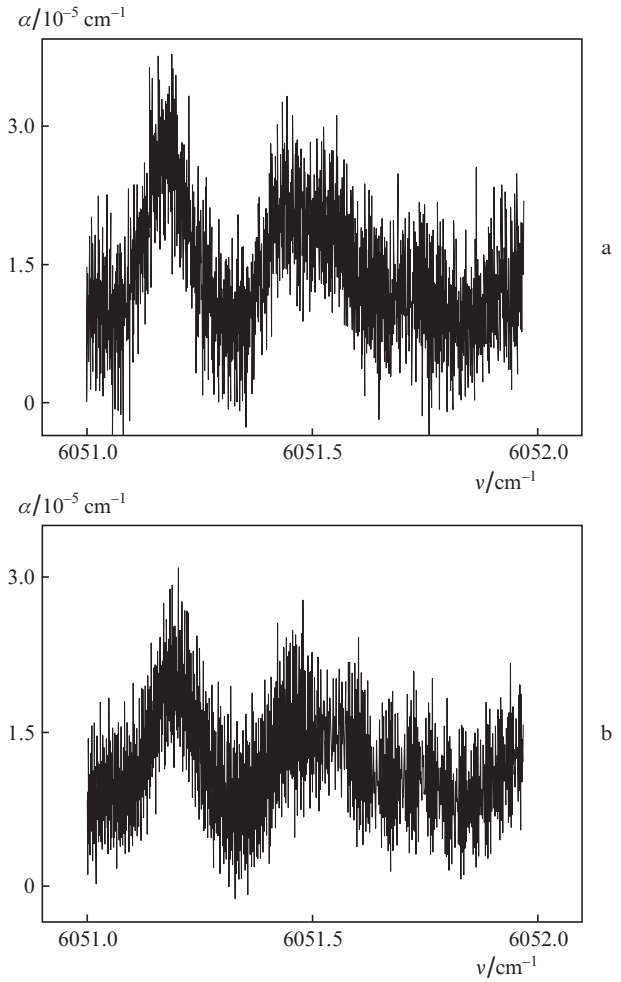

Figure 5. Absorption spectra of natural gas recorded by the R-ICOS method in a single laser scanning cycle of duration 5 ms (a) and by the conventional ICOS method with averaging over 1000 laser scanning cycles with the total signal accumulation time of 50 s (b).

of natural gas are shown. As in the previous case, the reflection coefficients of mirrors are 0.8. One can see that equal signal-to-noise ratios are observed in the R-ICOS method with a single frequency scanning cycle of duration 5 ms and in the ICOS method with 1000 cycles having a total signal acquisition time of 50 s.

In the conditions of our experiments, the rate and accuracy of recording spectra in the R-ICOS method were limited by capabilities of the ADC card (NI-6120, 16 bit, sampling rate 800 kHz). Spectra, recorded at the total number of samples 256 and 4096 corresponding to the entire range of laser frequency scanning, are shown in Fig. 6. The sampling time interval was 1.25 μs. One can see that a spectrum structure is well revealed already at a small number of sampling points. The time of recording a single spectrum was 320 μs in Fig. 6a and 5 ms in Fig. 6b.

Similar measurements have been performed with the resonator mirrors having a higher reflection coefficient of 0.99. In Fig. 7, results of fast recording the absorption spectrum with the same methane absorption line as in Fig. 4 are shown. In this case the resonator was filled with laboratory air. One can see a reliably detected absorption spectrum in the case of the R-ICOS method, whereas the ICOS method exhibits actually no absorption lines.

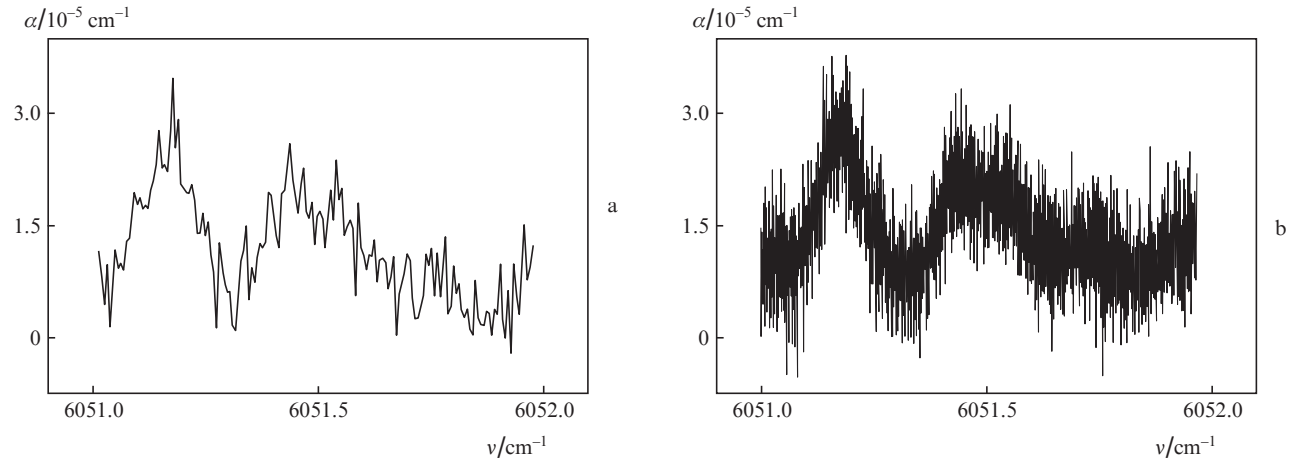

Figure 6. Absorption spectra of a natural gas mixture at various rates of laser frequency scanning: (a) 256 and (b) 4096 points per scan at the sampling time of 1.25 μs.

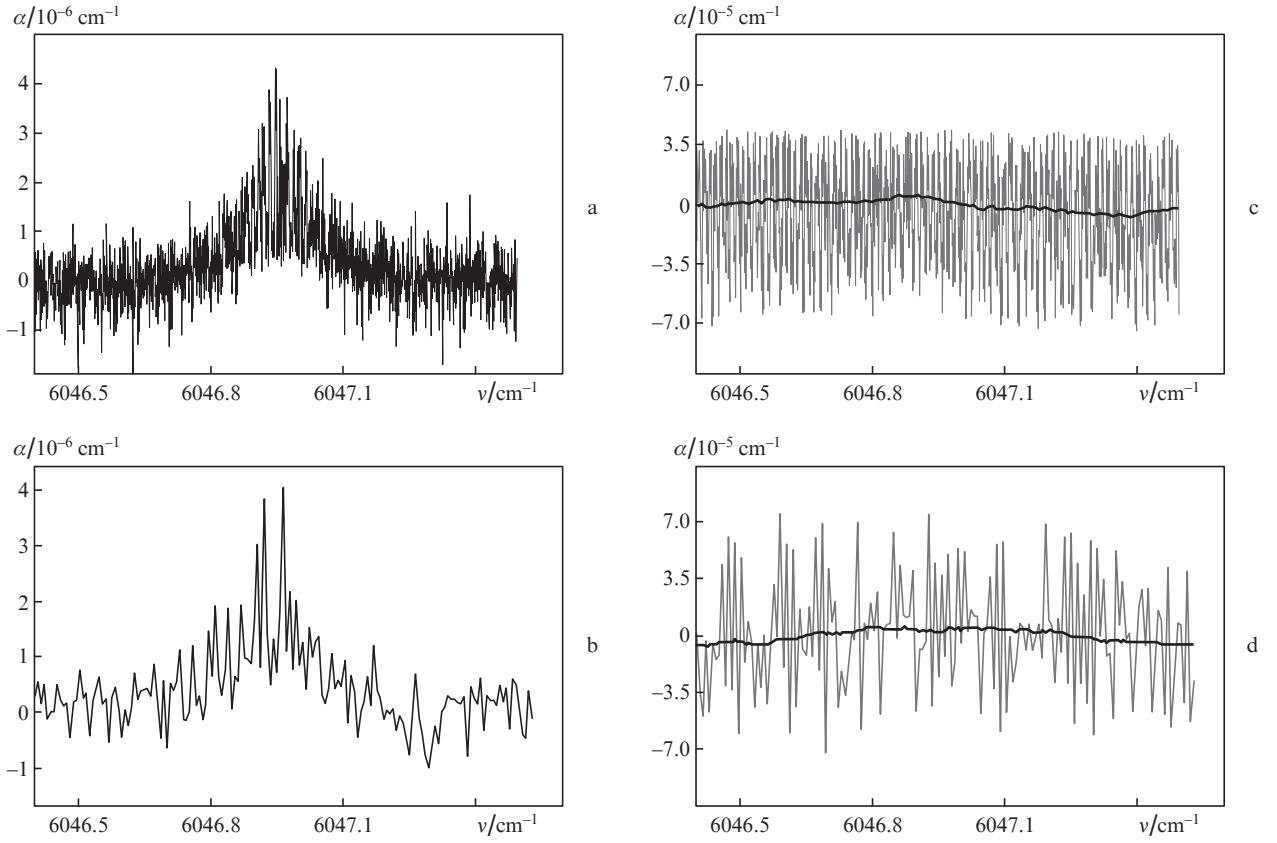

Figure 7. Absorption line in the spectrum of methane recorded by (a, b) the R-ICOS and (c, d) conventional ICOS methods at the recording time of 5 ms and the number of spectral points 4096 (a, c) and at the recording time of 320 μs and the number of spectral points 256 (b, d).

System sensitivity was estimated from the Allan variance plots $\sigma^2_{A\alpha}$ presented in Fig. 8 for the ICOS and R-ICOS methods in the conditions corresponding to Fig. 7.

Consider a correspondence between the ratios of variances for the R-ICOS and ICOS methods predicted in Section 2.3 and obtained experimentally. At an absorption index in the centre of the methane line in atmosphere $\alpha = 2\times10^{-6}$ cm^{-1} (Fig. 7) the ratio of variances predicted by formula (29) is $\sigma^2_{\text{ICOS}}/\sigma^2_{\text{RICOS}} = 5040$. However, in Fig. 8 one can see that the observed ratio of variances at short recording times is 500, i.e., the theoretical advantage is greater that the experimental. Such discrepancy can be explained by the fact that in addition to phase noise taken into account in the theoretical consideration, there are other types of noise in a measuring system.

Now we limit our consideration to short recording times where flickering and drift noises are not revealed and only white noise is present. The long-term stabilisation of the system is a specific problem not considered in the present work. From the theory and results of experiments in the conditions of the present work it follows that the new R-ICOS method suppresses noise much better than the ICOS method regardless of a particular ratio of noise levels in different methods.

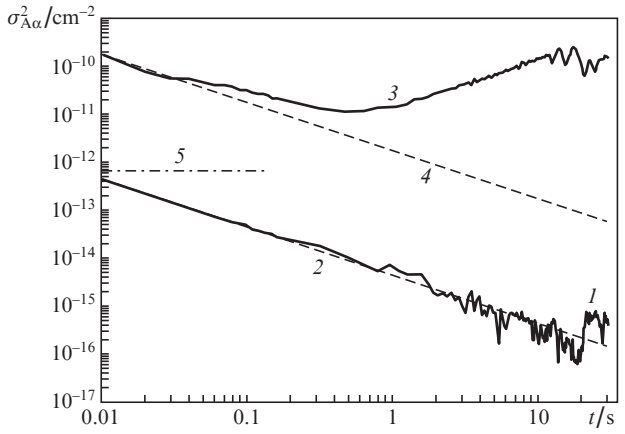

Figure 8. Allan variances $\sigma^2_{A\alpha}$ for methane absorption index (Fig. 7) measured by (*1*) the R-ICOS and (*3*) ICOS methods, Allan variances for the white noise level equivalent to the noise levels of signals in (*2*) the R-ICOS and (*4*) ICOS methods, and (*5*) absorption sensitivity corresponding to a background methane concentration in a standard atmosphere.

Since the new method eliminates just the phase noise one may assume that this type of noise makes a main contribution in the case of ICOS measurements, and noises of other types are relatively low. According to formulae (25) and (29), the phase noise is absent if there is no absorption ($\alpha \approx 0$). Hence, in the R-ICOS method, a noise trace in the far wing of an absorption line spectrum corresponds to noises that are not of phase nature. These may be amplitude noises of laser radiation, noise of photodetectors and electronic scheme, high-frequency vibrations of optical elements etc., i.e., noises arising in both the ICOS and R-ICOS methods.

In view of these facts we may introduce a variance σ_s^2 of these additional noises and add them to phase noises. A contribution of the additional noises into the total signal dispersion (24) in the case of ICOS method is negligible whereas their contribution into signal variance (25) in the case of R-ICOS at $\alpha \approx 0$ will be determining. The theoretical considerations given in Section 2.3 entail a simple conclusion that in such a limiting case in formula (29), instead of the ratio $\sigma^2_{ICOS}/\sigma^2_{RICOS}$ one may employ $\sigma^2_{ICOS}/\sigma_s^2$. By the amplitude of the noise trace in the wing of the absorption line in Fig. 4 one may estimate the variance of noises not related to a phase noise $\sigma_s^2 = 3\times10^{-13}$. In Fig. 8 one can see that at minimal recording times the variance is $\sigma^2_{ICOS} = 1.6\times10^{-10}$. Here, the ratio of noise variances $\sigma^2_{ICOS}/\sigma_s^2 \approx \sigma^2_{ICOS}/\sigma^2_{RICOS} \approx 530$, which is close to the observed value. Ratios of standard deviations for absorption indices of methane in atmosphere are given in Table 1.

One can see from Figs 7 and 8 that the sensitivity of the R-ICOS method is sufficient for detecting a background concentration of methane in standard atmosphere (1.7 ppm) even at the minimal recording time (320 μs) limited by capabilities of the electronic card employed for controlling the laser radiation and performing signal measurements. At a signal acquisition time of 20 s, a spectrum may be recorded with a sensitivity of up to 2×10^{-8} cm^{-1}. This value is substantially higher than that needed for carrying out ecological and medical investigations [19, 20].

Table 1. Calculated and measured ratios of standard deviations of absorption indices for methane in atmosphere.

Ratio of standard deviations	Calculation by formula (29)	Measured value	Calculation with additional noise taken into account ($\sigma_s^2 = 3\times10^{-13}$)
$(\sigma^2_{ICOS}/\sigma^2_{RICOS})^{1/2}$	70	22	–
$(\sigma^2_{ICOS}/\sigma_s^2)^{1/2}$	–	–	23

5. Conclusions

Possibilities of the new method of laser absorption spectroscopy R-ICOS for measuring weak absorption of radiation of a tunable laser in a gas medium placed in an external resonator by using additional light signal channels for the base line and for the radiation reflected from the resonator are studied. In the present work, main attention was paid to suppression of high-frequency noises which limit the sensitivity of the conventional integral single-beam ICOS method. It was shown that signal fluctuations caused by a mismatch between frequencies of laser radiation and resonator eigenmodes may be substantially suppressed. In order to compare possibilities of these methods, the theory of the R-ICOS method was developed and the theory of the known ICOS method was improved taking into account a finite spectral width of probe laser radiation. A higher sensitivity of the R-ICOS method predicted theoretically was confirmed experimentally.

The sensitivity of the suggested R-ICOS method in measuring an absorption index in a single cycle of fast spectrum scanning already exceeds by more than an order the sensitivity of the conventional ICOS method in the same experimental conditions. Absorption spectra of the background methane concentration in atmosphere were recorded in the range of diode laser radiation ~1650 nm. A minimal time needed for recording the spectrum in a single cycle of laser frequency scanning was 320 μs and was limited by capabilities of the electronic controlling and measuring system.

Due to suppression of phase noises the R-ICOS method can be employed with mirrors possessing moderate reflection coefficients. In the R-ICOS method, mirrors with the reflection coefficient of 0.99 provide measurements of methane concentration 40 times less than the background concentration in atmosphere at the acquisition time of 20 s. Sensitivity of measuring an absorption index in this case is 2×10^{-8} cm^{-1}. If the duration of scanning cycle is shorter than 1 ms, then the sensitivity is by 30–50 times worse; however, it is sufficient for measuring the background methane concentration.

The proposed method has clear prospects, which are as follows:

(i) Presently, commercial tunable diode lasers are available with the power comparable to that of the laser employed in the present work, but, with a generation line width of 100 kHz, which is approximately 100 times less than in our case. Employment of such lasers combined with highly reflecting mirrors may substantially improve the sensitivity and spectral resolution of the method without loss of performance.

(ii) Accuracy and sensitivity of the method may be increased by using known tricks in laser spectroscopy, including the wavelength modulation technique.

(iii) Higher performance and number of bits in digitising electronic signals will increase the sensitivity of the method.

These and other directions of developing the method require a more thorough study. In particular, the problem of long-term stability of the measuring system, which is important for designing devices based on this method, requires a

particular investigation. Certain directions on improvement of this parameter may be obtained by juxtaposing Allan variances (Fig. 8) and the results of our previous experiments [11, 12], where these variances were also studied, however, without absorption.

Acknowledgements. The work was supported by the Russian Foundation for Basic Research (Grant Nos 13-08-01188-a and 14-02-00553-a) and by the programme 'Fundamental Optical Spectroscopy and Its Applications' of Department of Physical Sciences RAS.

References

1. Ochkin V.N. *Spectroscopy of Low Temperature Plasma* (Weinheim: Wiley-VCH, 2009).
2. Herbelin J., McKay J., Kwok M., Ueunten R., Urevig D., Spencer D., Benard D. *Appl. Opt*., **19**, 144 (1980).
3. Berden G., Engeln R. *Cavity Ring-Down Spectroscopy: Techniques and Applications* (Chichester: Wiley, 2009).
4. Nikolaev I.V., Ochkin V.N., Peters G.S., Spiridonov M.V., Tskhai S.N. *Laser Phys*., **23**, 035701 (2013).
5. Engeln R., Berden G., Peeters R., Meijer G. *Rev. Sci. Instrum*., **69**, 3763 (1998).
6. O'Keefe A. *Chem. Phys. Lett*., **293**, 331 (1999).
7. O'Keefe A., Scherer J.J., Paul J.B. *Chem. Phys. Lett*., **307**, 343 (1999).
8. Paul J.B., Lapson L., Anderson J.G. *Appl. Opt*., **40**, 4904 (2001).
9. Korolenko P.V. *Opt. Spektrosk*., **30**, 271 (1971).
10. Engel G.S., Drisdell W.S., Keutsch F.N., Moyer E.J., Anderson J.G. *Appl. Opt*., **45**, 9221 (2006).
11. Nikolaev I.V., Ochkin V.N., Spiridonov M.V., Tskhai S.N. *Laser Phys*., **21**, 2088 (2011).
12. Nikolaev I.V., Ochkin V.N., Tskhai S.N. *Laser Phys. Lett*., **10**, 115701 (2013).
13. Born M., Wolf E. *Principles of Optics* (London: Pergamon, 1970; Moscow: Nauka, 1973).
14. Korolenko P.V. *Optika kogerentnogo izlucheniya* (Optics of Coherent Radiation) (Moscow: Izd. Mosk. Univ., 1998).
15. Andreev S.N., Nikolaev I.V., Ochkin V.N., Savinov S.Yu., Spiridonov M.V., Tskhai S.N. *Kvantovaya Elektron*., **37**, 399 (2007) [*Quantum Electron*., **37**, 399 (2007)].
16. Andreev S.N., Mironchuk E.S., Nikolaev I.V., Ochkin V.N., Spiridonov M.V., Tskhai S.N. *Appl. Phys. B*, **104**, 73 (2011).
17. http://zone.ni.com/reference/enXX/help/371361J01/lvanlsconcepts/general_ls_linear_fit_theory/.
18. *Atmosfera. Spravochnik* (Atmosphere. Handbook) (Leningrad: Gidrometeoizdat, 1991).
19. Kapitanov V.A., Tyryshkin I.S., Krivolutski N.P., Ponomarev Yu.N. *Opt. Atmos. Okean*., **17**, 617 (2004) [*Atmos. Ocean. Opt*., **17**, 553 (2004)].
20. Bingi V.N., Stepanov E.V., Chuhalin A.G., Milyaev V.A., Moskalenko K.L., Shulagin Yu.A., Yangurazova L.R. *Trudy IOF RAN*, **61**, 189 (2005).